Korean J. Chem. Eng., **30**(7), 1359-1367 (2013)
DOI: 10.1007/s11814-013-0083-y

REVIEW PAPER

Viruses as self-assembled nanocontainers for encapsulation of functional cargoes

Yuanzheng Wu*,, Hetong Yang**, and Hyun-Jae Shin*,†**

*Department of Chemical and Biochemical Engineering, Chosun University,
#375, Seosuk-dong, Dong-gu, Gwangju 501-759, Korea
**Biotechnology Center of Shandong Academy of Sciences, No. 19 Keyuan Road, Jinan 250014, China
(*Received 21 March 2013 • accepted 9 May 2013*)

Abstract−Viruses naturally exhibit an incredible variety of sophisticated nanostructures, which makes them ideal biological building blocks for nanoengineered material research. By mimicking their spontaneous assembly process, tremendous advances have been made towards utilizing virus and virus-like particles (VLPs) as protein cages, scaffolds, and templates for nanomaterials in the last few years. This review outlines recent progress in the field of bionanotechnology in which viruses are introduced to encapsulate various functional cargoes in a precise and controlled fashion. The encapsulation mechanisms are summarized into three main strategies: electrostatic interaction, chemical conjugation, and covalent attachment by genetic manipulation. The combination with chemical modification and genetic engineering heralds a brilliant future for fabrication of functional nanomaterials. These well-defined architectures will find attractive applications in biosensing, drug delivery, enzyme confinement, light-harvesting system, and pharmaceutical therapy.

Key words: Virus, Virus-like Particles (VLPs), Encapsulation, Nanomaterials, Drug Delivery

INTRODUCTION

Bionanotechnology, or nanobiotechnology, has become a rapidly developing area of science research for its tremendous applications [1]. Biological materials that display an astonishing variety of highly sophisticated architectures are appropriate nanostructures for new material development. Their prescribed shape together with the chemical and physical functionality provides huge advantages over other inorganic and organic substances [2]. Since the last decade, self-assembled natural protein complexes, such as viruses and virus-based nanoparticles (VNPs), ferritins [3], small heat shock protein [4], and enzyme complexes [5], have been employed as building blocks and templates in bionanotechnology. These bionanoparticles (BNPs) can form robust biosynthetic machineries while still being capable of modification by genetic and chemical approaches.

Viruses and noninfectious virus-like particles (VLPs) exhibit the characteristics of ideal building blocks for their exquisite symmetry, uniformity of size and shape, and precise assembly of hundreds of molecules into highly organized scaffolds [6]. They can undergo a reversible disassembly/reassembly process *in vivo* and *in vitro*. Chemical and genetic manipulations on the surface of viral protein cages confer unique properties to VLPs as programmable scaffolds in bionanotechnology [7]. The enclosed space in the interior of VLPs can encapsulate and release various functional moieties. Due to the well-defined structure and self-assembling system, a large number of VLPs have been elaborated to function as constrained reaction vessels, imaging agents, drug/gene delivery vehicles, and other nanomaterials. From the viewpoint of material scientists, viruses provide another type of widely studied biological macromolecules in nanometer scale, i.e., organic nanoparticles, which are composed of nucleic acids, capsid proteins, and sometimes envelopes [8].

Recently there have been some detailed reviews which summarize the remarkable progress of viruses or protein cages in biomedicine and nanomaterial research [9-11]. In this review, we focus on the encapsulation of functional materials by these viruses to illustrate their utilizations in nanotechnology.

VIRUS CAPSIDS

Historically studied for their effects as pathogens, viruses play a key role in biological systems as the most abundant biological entities on earth. Viruses especially lacking genomic nucleic acid are widely used as emerging platforms in bionanotechnology. These viruses exhibit a distinctive diversity of shapes and sizes, from simple helical and icosahedral forms to more complex structures, ranging between 20 and 750 nanometers. In this part various viruses and VLPs that have been studied in the field of nanotechnology will be presented (Fig. 1).

Icosahedral virus particles are nearly spherical and exhibit icosahedral symmetry in their arrangement [12]. The icosahedron is composed of equilateral triangles fused together into a closed shell, which generally has 20 facets and 12 vertices formed by one or several identical coat protein (CP) subunits (known as capsomers). The spherical lattices are collections of two-, three-, and fivefold rotation axes (5 : 3 : 2 symmetry). The protein shell usually assembles from 60- and 180-comma structures of pentamers and hexamers. The quasi-equivalence principle of protein subunits and their three-dimensional arrangement is illustrated by the triangulation (*T*) number, which was originally proposed by Caspar and Klug in 1962 [13]. Icosahedral viruses can self-assemble spontaneously into capsids with diameter about 20-80 nm, and the size of capsids depends on the

†To whom correspondence should be addressed.
E-mail: shinhj@chosun.ac.kr
‡This paper is dedicated to commemorate Prof. Ji-Won Yang (KAIST) for his retirement.

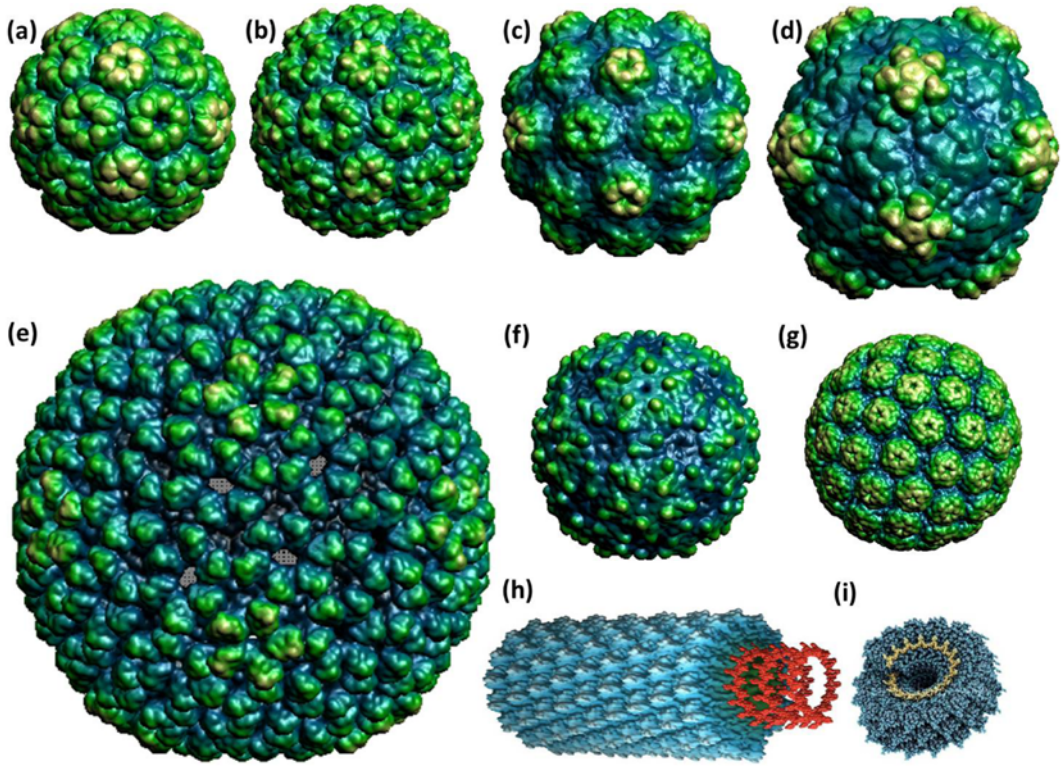

Fig. 1. Structures of virus particles used for nanotechnology. (a) Brome mosaic virus (BMV), 27 nm in diameter; (b) cowpea chlorotic mottle virus (CCMV), 28 nm in diameter; (c) turnip yellow mosaic virus (TYMV), 30 nm in diameter; (d) red clover necrotic mosaic virus (RCNMV), 36 nm in diameter; (e) bacteriophage P22, 58 nm in diameter; (f) bacteriophage MS2, 26 nm in diameter; (g) simian virus 40, 25 nm in diameter; (h) tobacco mosaic virus (TMV), 18 nm in diameter and variable in length; (i) top view of TMV. Structures (a)-(g) were obtained from the VIPER, URL: http://www.viperdb.scripps.edu/; TMV image by Jean-Yves Sgro, U. Wisconsin.

size and number of capsomers. The interior cavity of these cages offers the capacity to package genomic materials or encapsulate other particles.

Helical viruses are comprised of a single type of capsomer stacked around a central axis to form a helical structure, which results in a central cavity or hollow tube [12]. These viral helix arrangements are rod-shaped or filamentous, being either short and highly rigid or long and very flexible. The genetic material is enmeshed by the protein helix through interactions between the negatively charged nucleic acid and positive charged protein [14]. Helical particles are typically about 15-30 nm in diameter, and their lengths may range from 300 to 500 nm depending on the genome size.

Complex viruses usually have a combination of icosahedral and helical shape and contain extra appendages such as protein tails and/or complex exterior surfaces [12]. The head-tail structure comprising an icosahedral head bound to a helical tail is unique to bacteriophages that only infect bacteria. The poxvirus is one of the largest viruses and has a complex structure with an outer envelope with a thick layer of protein studded over its surface [15].

1. CCMV

Cowpea chlorotic mottle virus (CCMV) is a model plant virus belonging to the *Bromovirus* group of *Bromoviradea* family [16]. The capsid consists of 180 copies of a single protein (20 kDa, 190 amino acids) that form an icosahedral shell with an outer diameter of 28 nm and an inner diameter of 18 nm (T=3 symmetry). The quaternary structure of CCMV displays 32 prominent capsomers: 12 pentamers and 20 hexamers. CCMV was the first icosahedral virus to be reassembled *in vitro* into an infectious particle from wild-type purified components, i.e., the coat protein and genome RNA. The most profound property of CCMV is that the viral capsid can undergo a reversible structural transition depending on pH and ionic strength. The capsid expands into a radially swollen state around 10% when pH increases from 5.0 to 6.5 under low ionic strength (I<0.1 M). The swelling capsid with 60 separate open pores of 2-nm diameter permits ions to diffuse freely into and out of the cavity. The capsid then disassembles into protein dimers and RNA under high pH (above 7) and ionic strength (I~1 M). After removal of RNA and with a change in pH, the purified coat protein subunits will easily self-assemble and reform the capsids as shown in Fig. 2 [17]. This characteristic provides a unique molecular gating mechanism for entrapment of organic or inorganic materials and release of entrapped materials.

The high yield of CCMV capsid from natural infected leaf tissue (ca. 1-2 mg/g) capsid makes it suitable for the development of viral-based protein cage. Furthermore, heterologous expression of the coat protein in *Escherichia coli*, *Pseudomonas fluorescens*, and *Pichia pastoris* allows genetic alteration by site-directed mutagenesis. The wild and mutant-type of CCMV capsids are tolerant of high temperatures and various pH's, stable in organic solvents (e.g., DMSO), and nonpathogenic for mammals. These conspicuous properties enhance a wide range of chemical modification onto the capsid. The surface exposed amine (lysine), carboxylate (glutamate and aspartate), and thiol (cysteine) residues are accessible for attachment with

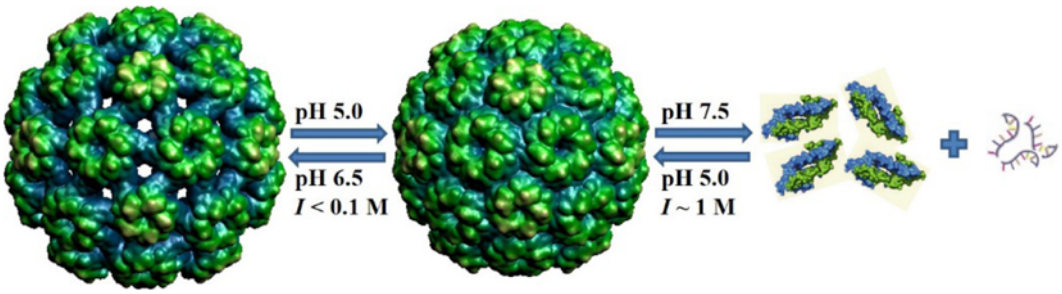

Fig. 2. Schematic representation of CCMV structure transition. With pH increasing from 5.0 to 6.5 under low ionic strength (I<0.1 M), CCMV capsid expands into a swollen state; when pH is increased to 7.5 under high ionic strength (I~1 M), the capsid disassembles into protein dimers and viral RNA. With/without the removal of RNA and pH lowering to 5.0, the protein dimers can be reassembled into empty/intact capsid.

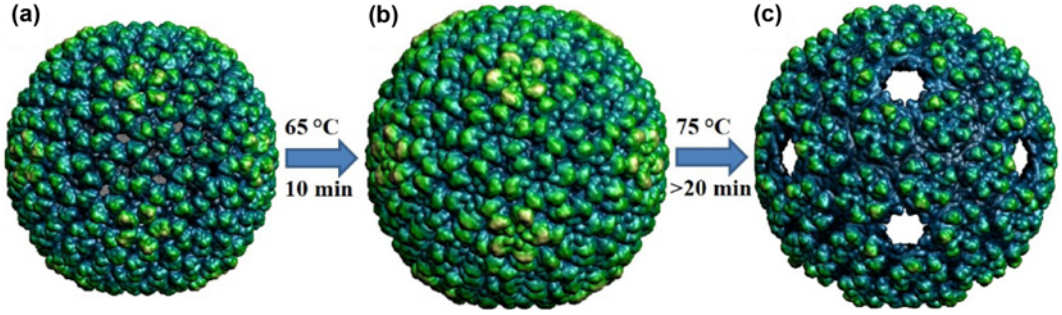

Fig. 3. Schematic representation of P22 structure transformation in three unique forms: (a) empty procapsid shell (ES) with a diameter of 58 nm; (b) mature capsid with a diameter of 64 nm after heating at 65 °C for 10 min; (c) wiffle-ball capsid (WB) after heating at 75 °C over 20 min.

specific ligands and small peptides via chemical interactions [16]. CCMV has feasible applications in biosensors, nanoelectric devices, and drug targeting and delivery.

2. Bacteriophage MS2

Bacteriophage MS2 is an icosahedral virus with an average diameter of 27 nm that infects *E. coli*. It contains one copy of maturation protein responsible for bacterial infection and 180 copies of coat protein (organized as 90 dimers) arranged into the phage head [18]. MS2 exhibits impressive stability to a broad range of temperature, pH, ionic strength, and organic solvent conditions. The coat protein can be propagated in multi-milligram quantities in bacteria by recombinant methods and afterwards be assembled to form empty VLPs. Genetically modified forms of MS2 are available for vaccine development and clinical diagnosis. Interestingly, MS2 also possesses 32 pores per capsid, each approximately 1.8 nm in diameter, which provides ready access to the interior space of moderately sized particles and reagents such as functionalized drug molecules for covalent attachment.

3. Bacteriophage P22

Salmonella typhimuriam bacteriophage P22 is an icosahedral virus assembled from 420 copies of coat protein with the assistance of approximately 300 copies of scaffolding protein (SP) [19]. The P22 capsid undergoes a structural transformation from the 58 nm empty procapsid shell (ES) to the mature capsid of 64 nm diameter (T=7) which is initiated by DNA packaging. The transformation can be mimicked *in vitro* by gentle heating (65 °C for 10 min). Further heating (75 °C over 20 min) produces a new form of wiffle-ball (WB) which has a 10 nm pore at each of the 12 icosahedral vertices caused by the release of subunits from the mature capsid (Fig. 3) [20]. The large pores of WB ensure free molecular exchange between the interior and exterior environments of the capsid. This unique characteristic makes the P22 capsid become a remarkable dynamic nanoplatform for synthetic utilization.

4. RCNMV

Red clover necrotic mosaic virus (RCNMV) is an icosahedral soil-transmitted virus with a diameter of 36 nm (T=3). The capsid of RCNMV is comprised of 180 copies of a 37 kDa coat protein packaging ssRNA [21]. The capsid has been demonstrated as a versatile container to entrap various nanoparticles in the diameter range 3-15 nm using RNA-dependent packaging based on the origin of assembly of RCNMV. Cryo-electron microscopy provides a molecular-level description of the mechanism whereby the RCNMV capsid undergoes a reversible opening and closure of pores at the pseudo-3-fold axes under control of divalent cations (Ca^{2+} and Mg^{2+}). Fluorescent dye and drug molecules have been incorporated into the interior cavity of RCNMV.

5. TMV

Tobacco mosaic virus (TMV), also known as tobamovirus, is a helical plant virus with a length of 300 nm and diameter of 18 nm. Its capsid is made from 2130 copies of coat protein arranged around the viral RNA [22]. The rod-like spiraling structure (16.3 proteins per helix turn) shows a distinct inner channel of 4 nm. Purified TMV coat protein undergoes a reversible states shift from micron-length rods in acetate buffer (pH 5.5) to double disks in phosphate buffer (pH 7.0). The internal and external surfaces of TMV capsid consist of repeated patterns of charged amino acid residues such as glutamate,

aspartate, arginine, and lysine that are viable for chemical ligation and bioconjugation [23]. TMV can be purified from infected tobacco plants in kilogram quantities. The particle is remarkably robust *in vitro*, remaining intact at temperatures up to 80 °C and pH values between 2 and 10. The assembled capsids have been used as templates to grow metal or metal oxide nanowires and coated conductive nanowires. TMV based materials offer a wide variety in the field of nanoelectronics, energy storage, and light harvesting.

MECHANISM OF ENCAPSULATION

The genomic RNA or DNA of virus is generally packaged within the capsid through a simple assembly and disassembly process *in vivo*. Scientists have discovered that a variety of phages, plant, and animal viruses can be assembled *in vitro* from their molecular components: proteins, nucleic acid, and sometimes lipids. Bancroft et al. first revealed the electrostatic interaction as the driving force for efficient packaging and assembly by encapsulation of polyanions instead of ssRNA inside icosahedral viruses [24]. The thermodynamic force during the assembly may include both specific and nonspecific interactions between the capsid and the genome, and there is no net delimitation to define these two mechanisms. The coat protein subunits themselves can spontaneously assemble into noninfectious VLPs under proper pH and ionic strength. From the viewpoint of material science, the highly uniform VLPs can be regarded as organic nanoparticles. The principle regulating the encapsidation of the genetic materials can also be utilized to load functional cargoes. The encapsulation occurs simply by mixing the protein subunits with cargo particles at specific ionic strength, temperature, and pH ranges. There have been numerous explorations in this respect, using viruses such as CCMV, brome mosaic virus (BMV), cucumber mosaic virus (CMV), RCNMV, hibiscus chlorotic ringspot virus (HCRSV) [25], simian virus 40 (SV40) [26], and bacteriophage MS2 (summarized in Table 1). The packaged functional cargoes include polymers, enzymes, liquid droplets, nucleic-acid functionalized particles, and even ligand-coated particles [27]. According to the encapsulation mechanisms, there are three main strategies, which will be discussed as follows.

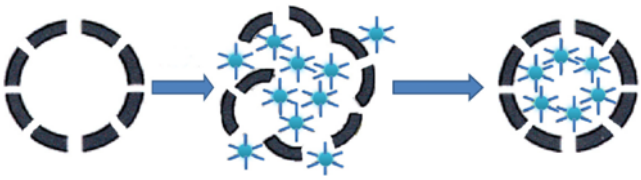

Fig. 4. Schematic diagram of encapsulation of foreign cargoes by viral capsids driven by electrostatic interaction. The negatively charged materials can act as the compressing genetic core to promote the assembly of a virus-like capsid as the natural type.

1. Electrostatic Interaction

The first strategy is to encapsulate the negatively charged species driven by electrostatic interaction (Fig. 4). The foreign material, for example, nanoparticles functionalized with anionic moieties or specific nucleic acid packaging signals and separated protein subunits, acts as the compressing genetic core to promote the assembly of a virus-like capsid like the natural type [28].

Douglas and Young first demonstrated the mineralization of two polyoxometalate species (paratungstate and decavanadate) and the encapsulation of an anionic polymer (poly-anetholesulphonic acid) inside CCMV capsids [29]. CCMV has been widely studied as a prominent example by several research groups for the ability to encapsulate various compounds. The exterior of the particle has a neutral charge, whereby the interior surface carries a high positive charge due to the presence of nine basic residues (arginine and lysine) on each subunit of coat protein. A straightforward way to entrap negatively charged molecules inside CCMV is to reversibly alter the pH to induce swelling and contraction of the capsid to facilitate the entry and sequestering of the foreign material. Nolte et al. further exploited the entrapment by CCMV with negatively charged polyelectrolytes including poly (styrene sulfonate) (PSS), polyferrocenylsilane (PFS), and poly[(2-methoxy-5-propyloxy sulfonate)-phenylene vinylene] (MPS-PPV) [30,31]. The encapsidation can lead to monodisperse or polydisperse formation of T=1, 2, and 3 VLPs. These

Table 1. Summary of viral capsids used for the encapsulation study

Encapsulation mechanism	Viral capsids	Encapsulated cargoes [Ref.]
Electrostatic interaction	CCMV	Polyoxometalate, polyelectrolytes, enzymes [29-31,35]
	TMV	CdS, PbS, silica, and iron oxide [32]
	BMV	PEGylated gold nanoparticles [33]
	RCNMV	Au and $CoFe_2O_4$ nanoparticles, Quantum dots (Qds) [34]
Chemical conjugation	TMV	The interior glutamate residues coupled by carbodiimide reaction [37]
	Bacteriophage MS2	The interior tyrosine residues coupled with diazonium salt of *p*-nitroaniline [38]
	Rotavirus VP6	The interior carboxyl groups coupled with the amine groups of DOX [39]
Covalent attachment by genetic manipulation	CCMV	The K-coil-modified capsids interacted with E-coil-EGFP by coiled-coil linkers [41]
	JC virus	The installed hexahistidine motif (His_6GFP) specifically binded with nitrilotriacetic acid-sulforhodamine (NTA-SR) by His_6-tag affinity [45]
	Bacteriophage P22	Cysteine residues introduced on valine 119 (V119C), lysine 110 (K110C) and lysine 118 (K118C), bioconjugated with maleimide-PEO_2-biotin (MPB) [42]
	Bacteriophage MS2	Cysteine residues introduced on asparagine 87 (N87C), bioconjugated with Alexa Fluor 488 maleimide [43]

approaches could be utilized for the encapsulation of negatively charged drug molecules for pharmaceutical applications in future.

Interestingly, the internal mineralization of CdS, PbS, silica, and iron oxide using TMV capsids, which led to the template-directed synthesis of inorganic-organic nanotubes, was also achieved [32]. The inner surface of TMV showed a high spatial density of glutamic acid residues, suggesting that nucleation within the 4 nm wide inner channel might have been expected under these conditions. The virus-based hybrid nanomaterials hold promise for development as platforms for the creation of hybrid materials with engineering applications such as nanowires and catalysts.

Dragnea et al. have shown that PEGylated gold nanoparticle could act as nucleating core for the self-assembly of BMV capsid, and the size of the formed hybrid VLPs was proportional to the size of anionic polymer cargoes [33]. The artificial core mimicked the process to promote the assembly of a symmetric viral protein structure around it in the absence of genomic RNA. The nonspecic core/capsid interactions were predominant during the assembly of forming capsid. The encapsulation efciency depended on the nanoparticle size, with a maximum efficiency occurring for 12 nm gold nanoparticles. The initial CP to Au particle ratio (CP/Au) with a threshold value above 100 protein subunits per gold nanoparticle was required for a complete capsid. VLPs of varying diameters were found to resemble three classes of viral particles (T=1, 2, and 3) the same way as the wild type of BMV: T=1 BMV capsids (60 CP) was obtained for 6 nm nanoparticle cores, while 12 nm particle cores promoted the formation of T=3 capsids (180 CP).

However, the encapsulation of various nanoparticles by RCNMV was found to yield uniform sized VLPs, independent of the composition and sizes of cores, which ranged from 3 to 15 nm [34]. Apart from the electrostatic interaction between coat protein and genomic RNA, the assembly of RCNMV requires a unique hairpin structure within RNA-2 hybridized with RNA-1 to form the origin of assembly (OAS) for selective recruitment and orientation of CP subunits. An oligonucleotide mimic of the OAS sequence was attached to Au and $CoFe_2O_4$ nanoparticles and Quantum dots (Qds), followed by addition of RNA-1 to form a synthetic OAS to initiate VLPs assembly. Despite the different type and size of packaged nanoparticles, the formed VLPs were homogeneous in size with an average diameter of 32.8 nm, less than that of the native virus at 36.6 nm.

Another fascinating exploration of virus encapsidation is to incorporate individual horseradish peroxidase (HRP) in the inner cavity of CCMV capsid for single enzyme studies [35]. Using the pH-dependent disassembly/reassembly process, HRP was loaded and immobilized in the capsid with only one or no enzyme present per capsid. The fluorogenic substrate dihydrorhodamine 6G diffused in the HRP-containing CCMV capsid where HRP catalyzed the oxidation of this non-fluorescent substrate to produce rhodamine 6G The release of fluorescent product through the pores on the capsid was easily monitored by confocal fluorescence microscope. The spatially confined virus capsid contributes to the understanding of the behavior and the interactions of enzymes at the single-molecule level.

2. Chemical Conjugation

The second strategy is to package the reagents or cargo molecules by chemical conjugation with the coat protein subunit as presented in Fig. 5. The foreign material is first transported and then sequestered inside the capsid by covalent bond such as peptide (amide) bonds between the carboxylate groups of amino acid residues and the amine groups of cargo molecules [36]. The chemically well-defined local environment of the viral cavity provides the circumstance to directly synthesize inside the capsid.

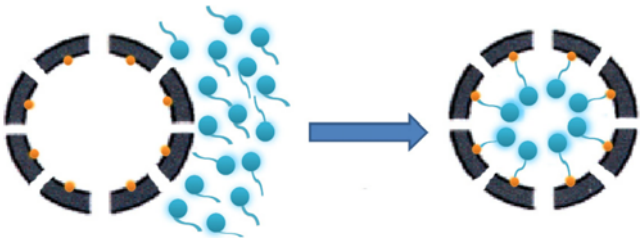

Fig. 5. Schematic diagram of encapsulation of foreign cargoes by viral capsids based on chemical conjugation. The cargo molecules (blue) interact with the functional groups of amino acid residues on the interior of capsids (orange) by covalent bond such as peptide (amide) bonds.

Francis et al. used rod-shaped TMV capsid as a robust and practical scaffold for the preparation of nanoscale materials [37]. Both the exterior and the interior surface of the virus were attached with new functionality strategies separately. As for the inner cavity of TMV, the modification strategy focused on glutamate residues as targets for amide bond by a carbodiimide coupling reaction with 1-ethyl-3-(3-dimethyl-aminopropyl) carbodiimide (EDC). Glu 97 exposed on the core surface was identified as the primary site of modification and Glu 106 was also found with appreciable reactivity, while there was no modification of exterior aspartic acids and carboxy terminus observed. After disassembly/reassembly process the internally modified TMV conjugates revealed rod-shape structures that were virtually identical to the native capsids. Importantly the interior surface could also be doubly modified by rhodamine derivative conjugation with azo-modified capsids, yielding ~650 internal chromophores per 300 nm rod. This method positioned the new functional groups as closely as 1 nm apart on the inside of TMV capsid. Different functional groups were eventually installed on the exterior and interior surfaces of the same capsid assemblies.

Bacteriophage MS2 was also modified using same covalent strategy to load drug molecules and imaging agents. The tyrosine 85 residue located on the interior face of each monomer after capsid assembly could be functionalized by a rapid and efficient coupling with the diazonium salt of *p*-nitroaniline. 50-70 copies of a fluorescent dye (5-amino-N-(2-[FAM-amido]-ethyl)-2-nitrobenzamide) were installed to the phenolic moiety of the tyrosine through the *ortho* azo linkage to serve as visualization probes for subsequent cell-based assays. After decoration of the exterior surface with PEG chains, biotin groups were then placed at the distal ends of the polymer chains to bind with streptavidin. Despite all these high levels of modification, MS2 capsids remained in the assembled state [38]. This modular strategy was developed to attach small targeting molecules on virus capsids for the potential therapeutic delivery.

More recently, the self-assembled rotavirus (RV) VLPs by the major viral protein VP6 were chemically conjugated with an anticancer drug doxorubicin (DOX) [39]. The formation of amide bond between the carboxyl group of VP6 and the amine group of DOX

was achieved in the presence of EDC and N-hydroxysuccinimide (NHS). There are six carboxylate groups on each VP6 subunit exposed on the exterior surface and seven carboxylate groups on the interior surface. For the DOX-loaded VLPs (DVLPs) it was estimated that about 12 DOX molecules were bound to each VP6 protein, meaning that most carboxylate groups on both surfaces were chemically occupied. DVLPs were further linked by lactobionic acid (LA) as target for hepatocytes or hepatoma cells bearing asialoglycoprotein receptors (ASGPRs). LA-modified DVLPs (DVLPLAs) showed specific immunofluorescence in HepG2 cells *in vitro*. The release of DOX from DVLPLAs was simulated under lysosomal conditions, and there was little release without protease in presence. This indicated it was suitable for transportation in the bloodstream (pH close to 7.4). The chemically functionalized VLPs may find practical applications in biomedicine.

3. Covalent Attachment by Genetic Manipulation

The third strategy is to integrate the cargo molecules based on covalent attachment with the site-specific residues on the capsid protein which is engineered through genetic manipulation (Fig. 6). The gene modification of coat protein results in the alteration of the amino acid residues displayed on the interior of the virus cage and even the charge change of the interior surface, which then offers functional versatility amenable to the chemical coupling with target peptides or other cargoes [40].

Making use of heterodimeric coiled-coil linkers, Cornelissen et al. reconstructed the interior cage of CCMV and encapsulated positively charged proteins inside it [41]. The K-coil $(KIAALKE)_3$ with positively charged lysine was introduced at the N-terminus of CCMV CP and E-coil $(EIAALEK)_3$ with negatively charged glutamic acid at the C-terminus of the enhanced green fluorescent protein (EGFP) and the modified proteins were expressed in *E. coli*, respectively. Specific heterodimerization between K-coil and E-coil led to the formation of EGFP-CP complex. After the assembly of EGFP-CP complex with wild-type CP, EGFP-filled capsids were obtained. Depending on the concentration and ratio of EGFP-CP/wt CP, up to 15 EGFP proteins were encapsulated per capsid. This provides a brand new approach of modification on virus capsids by gene manipulation.

Bacteriophage P22 is another virus that has been genetically manipulated to enhance the ability to package programmed cargoes [42]. Three residues of coat protein located on the interior surface were genetically substituted with cysteine residues: valine 119 (V119C) in the middle of the hydrophobic face, lysine 110 (K110C) in the middle of the hydrophilic face, and lysine 118 at the helical border (K118C). Maleimide-PEO_2-biotin (MPB), with a thiol reactive maleimide on one end and a biotin affinity tag to recruit reacting partners of streptavidin (StAv) on the other end, was site-specifically attached with the two morphological types (procapsid shell, ES form and wiffle-ball, WB form) of three mutants. Neither form of V119C was labeled with MPB, suggesting that C119 is not available in either form. While almost all subunits of K110C were labeled with MPB in ES form and completely blocked in WB form, indicating that C110 is only accessible in ES form. Only 35% of subunits of K118C in ES were labeled with MPB, whereas all the subunits were labeled in WB, showing that the partially exposed C118 becomes fully exposed to the interior surface during structural transformation from ES to WB.

Bacteriophage MS2 also presents a readily available scaffold for the construction of targeted delivery agents by genetic modification [43]. Wild type MS2 contains two native cysteines on the interior surface which are inaccessible under normal maleimide bioconjugation conditions. Therefore, a cysteine residue was introduced at asparagine 87 (N87C) of the coat protein. The mutation provided 180 sulfhydryl groups on the interior surface for cargo installation. Through the cysteine alkylation reaction, Alexa Fluor 488 maleimide was encapsulated as fluorescent label. 20-40 copies of 41-nucleotide DNA aptamers that target protein tyrosine kinase 7 (PTK7) receptor on Jurkat T cells were then installed on the outer surface of MS2 shell. The capsids bearing the cell-targeting sequence showed significant binding to Jurkat cells. These suggested that aptamer-labeled capsids could be used as convenient and evolvable targeting groups for drug delivery.

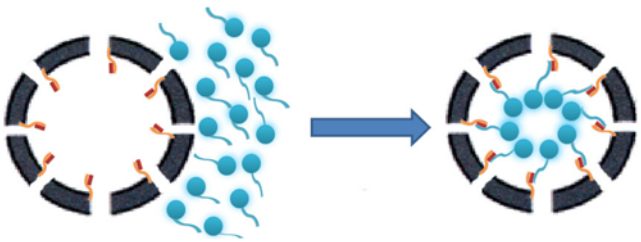

Fig. 6. Schematic diagram of encapsulation of foreign cargoes by viral capsids through genetic manipulation. The additional motifs (red) can be introduced inside virus cages by gene modification, which are amenable to cargo molecules (blue) by specific chemical coupling.

APPLICATIONS

1. Drug Delivery

With excellent biocompatibility and biodegradability, there are

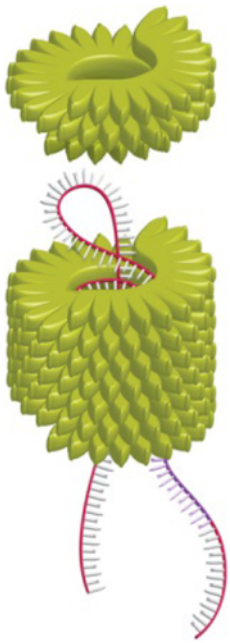

Fig. 7. Schematic representation of TMV-based siRNA formation for gene delivery.

various potential applications of functional self-assembled virus-based materials. Bentley's team has successfully utilized the hollow capsid of TMV as an RNAi carrier for gene delivery into mammalian and insect cells (Fig. 7) [44]. RNA interference (RNAi), which is a process in which RNA molecules reduce gene expression by causing the destruction of specific mRNA molecules, usually involves two small RNA molecules: microRNA (miRNA) and small interfering RNA (siRNA). There is an OAS within TMV genomic RNA which forms a unique hairpin structure and associates with coat protein to initiate the assembly. By incorporating TMV OAS into a siRNA which can program cells to destroy disease-causing proteins, the siRNA could assemble into "pseudo-virions" with coat protein. To deliver the siRNA to the targeted cells, pseudo virions are further modified with synthetic cell-penetrating peptides to facilitate cell endocytosis. The results showed pseudo virions targeting cyclin E (antisense cycE) were capable of arresting cells at G1 phase. TMV can be traced in the blood of most people from second-hand smoke and does not seem to cause irritation or obvious immune-system problems. This TMV-based siRNA packaging system protects the frail siRNA from degradation and provides a means of delivering RNAi constructs into various host cells. Through changing the types of siRNA, multiple diseases from cancers to genetic disorders could be targeted and treated by this therapeutic agent in the future.

A pH-dependent drug release system has been developed based on the JC virus, a type of human polyomavirus, by Ijiro et al. [45]. Green fluorescence protein with N-terminal hexahistidine motif (His_6GFP) was fused to the N-terminus of the inner core protein VP2 (His_6GFP-VP2) and co-expressed with the major coat protein VP1 in *E. coli*. VP1 and His_6GFP-VP2 associated with each other and formed His_6GFP-incorporated VLPs (His_6GFP-VLPs) with a diameter of 52.4±7.1 nm. Nitrilotriacetic acid-sulforhodamine (NTA-SR), containing both a His_6-tag-targeting NTA segment and a fluorescent sulforhodamine segment, could be encapsulated within His_6GFP-VLPs through the 1 nm holes at pH 7.4 and bind specifically to the His_6 tags. NTA was then released from the His_6GFP-VLPs at pH 5.0 due to a decrease in His_6-tag affinity, which has similar pH to the endosome and the lysosome. The process resulted in saturation of release within 20 min. The controlled release of GFP was further examined using NIH3T3 cells. In this system, VP2 acted as an anchoring unit for the protonation of histidines, which could offer specific and reversible attachment of drug molecules. The feasibility of the encapsulation-release system can be used as a cell-specific drug delivery vehicle.

2. Enzyme Nanocontainer

The virus capsid provides a well-defined structure to encapsidate the enzyme in a spatially confined way to observe the catalytic activity even in single-molecule level. The entrapment of enzymes in virus capsids has been done in CCMV, MS2, et al. A precise number of enzyme *Pseudozyma antarctica* lipase B (PalB) loaded into CCMV capsid were accomplished based on a coiled-coil linker described in Section 3.3 and EGFP was co-encapsulated as a non-catalytic protein to investigate the reaction rate [46]. The apparent overall reaction rate increased upon encapsulation and was almost independent of the number of enzymes in the capsid. The encapsulated PalB seemed to have a higher activity than non-encapsulated PalB. It was more likely caused by extremely high confinement molarity (M_{conf}=~1 mM) of the enzyme combined with an increased collision chance due to the spatial confinement leading to very rapid formation of the enzyme-substrate complex. These results highlight the importance of small volumes for efcient multi-enzyme cascade catalysis.

The RNA-removed MS2 capsids were also used to encapsulate *E. coli* alkaline phosphatase (PhoA) [47]. To increase the yield of encapsulation, PhoA was tagged with a 16 acidic peptide at C-terminus (PhoA-neg); trimethyl amine N-oxide (TMAO) was added as an osmolyte to decrease protein unfolding and increase the thermal stability. After incubation of PhoA-neg with disassembled coat protein dimers under presence of TMAO, intact capsids with the diameter of 27 nm were observed. About 1.6 PhoA-neg dimers were packaged per capsid. Enzyme assay was monitored by the hydrolysis of 4-methylumbelliferyl phosphate to yield fluorescent 4-methylumbelliferone. The value of K_m was equal to that of the free enzyme dimer and the K_{cat} was slightly reduced when the enzyme was encapsulated, possibly due to the constrained enzyme environment. This method provides a practical and potentially scalable way of studying the complex effects of encapsulating enzymes in protein-based compartments.

3. *In Vivo* Imaging

Near infrared (NIR) fluorescence imaging based upon virus capsids is particularly advantageous in optical imaging and therapy of disease. Indocyanine green (ICG), an FDA-approved NIR chromophore, was encapsulated into BMV for the utilization of mammalian intracellular optical imaging [48]. Instead of genomic RNA, the negatively charged ICG interacted with the positively charged arginine-rich motif in the N-terminus of BMV CP subunits to assemble into optical viral ghosts (OVGs). The mean diameter of OVGs was ~24.3 nm in T=1 symmetry. OVGs maintained stable at the absorption spectrum of ICG in the 600-900-nm NIR range and reduced by ~15% for 3 h at 37 °C. Human bronchial epithelial (HBE) cells were used to detect the intracellular optical imaging of OVGs, with the result that OVGs were internalized and localized at more than 90% of the HBE cells after 3 h. These constructs may serve as a potentially nontoxic and multifunctional nanoplatform for site-specific deep-tissue optical imaging and therapy of disease.

4. Light-harvesting System

A virus-based approach has been developed as light-harvesting systems through self-assembly. Recombinant TMV CP monomers with a reactive cysteine residue were constructed for the thiol-reactive chromophore attachment [49]. Three chromophores were installed on the interior surface of TMV including Oregon Green 488 maleimide as the primary donor, tetramethylrhodamine maleimide as an intermediate donor, and Alexa Fluor 594 maleimide as the acceptor. The conjugated TMV VLPs could be assembled into stacks of disks or rods under different buffers. Under both morphologies, there was efficient energy transfer (over 90% overall efficiency) observed using fluorescence spectroscopy, from numbers of donor chromophores to a single acceptor. Later, multiple porphyrin arrays were accomplished similarly in TMV, in which Zn-porphyrin (ZnP) was coordinated as donor and free-base porphyrin (FbP) as acceptor [50]. The photophysical properties of the arrayed porphyrins in the TMV assemblies were examined by time-resolved fluorescence spectroscopy, and the energy transfer rates were determined to be 3.1-6.4×10^9 s^{-1}. CCMV capsids were also employed to package and syn-

thesize TiO_2 nanoparticles, which showed similar structure to nanocrystalline anatase and photocatalytic activity [51]. This highly tunable method has emerged for the construction of photovoltaic devices.

CONCLUSION AND OUTLOOK

The ability to precisely encapsulate components into virus capsids by self-assembly, chemical conjugation, or genetic manipulation has inspired the creation of complex systems with novel functions. However, we should not just focus on one side of the coin. Today there are two main trends in the fabrication of modified virus capsids for nanotechnology: surface modification and encapsulation [52]. The selective chemical derivatization of viral exterior surface that allows the attachment of fluorescent dyes, gold clusters, and specific moieties has been demonstrated permissible in myriad viruses, e.g., cowpea mottle virus (CPMV) was exploited as addressable nanoblocks which can be imbued with a variety of chemical and physical properties [53].

As mentioned, the combination of two methods turns out to be more delicate and efficient for practical utilization. The chemical addressability of exterior and interior surfaces of virus capsids by covalent bioconjugation such as diazonium coupling and Cu(I)-catalyzed azide-alkyne cycloaddition (CuAAC) reaction [54] provides a diversity of functional moieties of versatile repertory. These dual modified VLPs can specifically recognize certain types of cells, attach with corresponding receptors, and deliver the packaged cargoes into the endosome.

Furthermore, quite a few plant viruses such as CCMV, CPMV, TMV, and rodlike phages have been shown to be noninfectious to humans and mammals in general, and will not induce obvious toxicity and immune response in human beings [55]. These will be quite promising nanocarriers with some issues concerning the toxicity and immunology to be fully evaluated. Virus particles have presented distinguished stability and flexibility for pharmaceutical application, biomaterial fabrication, and photovoltaic construction. More light will be cast upon these elegant and elaborate creations in the future.

ABBREVIATIONS

BMV : brome mosaic virus
BNPs : bionanoparticles
CCMV : cowpea chlorotic mottle virus
CMV : cucumber mosaic virus
CP : coat protein
CPMV : cowpea mottle virus
CuAAC : Cu(I)-catalyzed azide-alkyne cycloaddition
DOX : doxorubicin
EDC : 1-ethyl-3-(3-dimethyl-aminopropyl) carbodiimide
EGFP : enhanced green fluorescent protein
ES : empty procapsid shell
FbP : free-base porphyrin
HBE : human bronchial epithelial
HCRSV : hibiscus chlorotic ringspot virus
HRP : horseradish peroxidase
ICG : indocyanine green
LA : lactobionic acid
miRNA : microRNA
MPB : maleimide-PEO_2-biotin
MPS-PPV : poly[(2-methoxy-5-propyloxy sulfonate)-phenylene vinylene]
NHS : N-hydroxysuccinimide
NIR : near infrared
NTA-SR : nitrilotriacetic acid-sulforhodamine
OAS : origin of assembly
OVGs : optical viral ghosts
PalB : *Pseudozyma antarctica* lipase B
PFS : polyferrocenylsilane
PhoA : *E. coli* alkaline phosphatase
PSS : polystyrene sulfonate
PTK7 : protein tyrosine kinase 7
Qds : Quantum dots
RCNMV : red clover necrotic mosaic virus
RNAi : RNA interference
RV : rotavirus
siRNA : small interfering RNA
SP : scaffolding protein
StAv : streptavidin
SV40 : simian virus 40
TMAO : trimethyl amine N-oxide
TMV : tobacco mosaic virus
VLPs : virus-like particles
VNPs : virus-based nanoparticles
VP : viral protein
WB : wiffle-ball
ZnP : Zn-porphyrin

REFERENCES

1. C. M. Soto and B. R. Ratna, *Curr. Opin. Biotechnol.*, **21**, 426 (2010).
2. J. M. Kim, S. M. Chang, H. Muramatsu and K. Isao, *Korean J. Chem. Eng.*, **28**, 987 (2011).
3. T. Ueno, M. Suzuki, T. Goto, T. Matsumoto, K. Nagayama and Y. Watanabe, *Angew. Chem. Int. Ed.*, **43**, 2527 (2004).
4. K. K. Kim, R. Kim and S. H. Kim, *Nature*, **394**, 595 (1998).
5. G. J. Domingo, S. Orru and R. N. Perham, *J. Mol. Biol.*, **305**, 259 (2001).
6. J. Rong, Z. Niu, L. A. Lee and Q. Wang, *Curr. Opin. Colloid Interface Sci.*, **16**, 441 (2011).
7. J. K. Pokorski and N. F. Steinmetz, *Mol. Pharm.*, **8**, 29 (2011).
8. G. Lee, Y. S. Cho, S. Park and G. R. Yi, *Korean J. Chem. Eng.*, **28**, 1641 (2011).
9. T. Douglas and M. Young, *Science*, **312**, 873 (2006).
10. K. T. Kim, S. A. Meeuwissen, R. J. Nolte and J. C. van Hest, *Nanoscale*, **2**, 844 (2010).
11. K. J. Koudelka and M. Manchester, *Curr. Opin. Chem. Biol.*, **14**, 810 (2010).
12. D. M. Knipe and P. M. Howley, *Fields Virology*, 5th Ed., Lippincott Williams & Wilkins, Philadelphia (2007).
13. D. L. Caspar and A. Klug, *Cold Spring Harb Symp. Quant. Biol.*, **27**, 1 (1962).
14. M. A. Hemminga, W. L. Vos, P. V. Nazarov, R. B. Koehorst, C. J. Wolfs, R. B. Spruijt and D. Stopar, *Eur. Biophys. J.*, **39**, 541 (2010).
15. C. Gubser, S. Hué, P. Kellam and G. L. Smith, *J. Gen. Virol.*, **85**, 105

(2004).
16. J. A. Speir, S. Munshi, G. Wang, T. S. Baker and J. E. Johnson, *Structure*, **3**, 63 (1995).
17. F. Tama and C. L. Brooks III, *J. Mol. Biol.*, **318**, 733 (2002).
18. K. Valegard, L. Liljas, K. Fridborg and T. Unge, *Nature*, **36**, 345 (1990).
19. M. H. Parker, S. Casjens and P. E. Prevelige Jr., *J. Mol. Biol.*, **281**, 69 (1998).
20. C. M. Teschke, A. McGough and P. A. Thuman-Commike, *Biophys. J.*, **84**, 2585 (2003).
21. L. Tang, *Nat. Struct. Biol.*, **8**, 77 (2001).
22. A. Klug, *Philos. Trans. R. Soc. Lond. B Biol. Sci.*, **354**, 531 (1999).
23. M. Demir and M. H. Stowell, *Nanotechnology*, **13**, 541 (2002).
24. J. B. Bancroft, E. Hiebert and C. E. Bracker, *Virology*, **39**, 924 (1969).
25. F. Li, Z. P. Zhang, J. Peng, Z. Q. Cui, D. W. Pang, K. Li, H. P. Wei, Y. F. Zhou, J. K. Wen and X. E. Zhang, *Small*, **5**, 718 (2009).
26. Y. Ren, S. M. Wong and L. Y. Lim, *J. Gen. Virol.*, **87**, 2749 (2006).
27. Y. Ma, R. J. Nolte and J. J. Cornelissen, *Adv. Drug Deliv. Rev.*, **64**, 811 (2012).
28. S. E. Aniagyei, C. DuFort, C. C. Kao and B. Dragnea, *J. Mater. Chem.*, **18**, 3763 (2008).
29. T. Douglas and M. Young, *Nature*, **393**, 152 (1998).
30. F. D. Sikkema, M. Comellas-Aragonès, R. G. Fokkink, B. J. Verduin, J. J. Cornelissen and R. J. Nolte, *Org. Biomol. Chem.*, **5**, 54 (2007).
31. M. Brasch and J. J. Cornelissen, *Chem. Commun.*, **48**, 1446 (2012).
32. W. Shenton, T. Douglas, M. Young, G. Stubbs and S. Mann, *Adv. Mater.*, **11**, 253 (1999).
33. M. C. Daniel, I. B. Tsvetkova, Z. T. Quinkert, A. Murali, M. De, V. M. Rotello, C. C. Kao and B. Dragnea, *ACS Nano*, **4**, 3853 (2010).
34. L. Loo, R. H. Guenther, S. A. Lommel and S. Franzen, *J. Am. Chem. Soc.*, **129**, 11111 (2007).
35. M. Comellas-Aragonès, H. Engelkamp, V. I. Claessen, N. A. Sommerdijk, A. E. Rowan, P. C. Christianen, J. C. Maan, B. J. Verduin, J. J. Cornelissen and R. J. Nolte, *Nat. Nanotechnol.*, **2**, 635 (2007).
36. M. Uchida, M. T. Klem, M. Allen, P. Suci, M. Flenniken, E. Gillitzer, Z. Varpness, L. O. Liepold, M. Young and T. Douglas, *Adv. Mater.*, **19**, 1025 (2007).
37. T. L. Schlick, Z. Ding, E. W. Kovacs and M. B. Francis, *J. Am. Chem. Soc.*, **127**, 3718 (2005).
38. E. W. Kovacs, J. M. Hooker, D. W. Romanini, P. G. Holder, K. E. Berry and M. B. Francis, *Bioconjug. Chem.*, **18**, 1140 (2007).
39. Q. Zhao, W. Chen, Y. Chen, L. Zhang, J. Zhang and Z. Zhang, *Bioconjug. Chem.*, **22**, 346 (2011).
40. L. A. Lee, Z. Niu and Q. Wang, *Nano Res.*, **2**, 349 (2009).
41. I. J. Minten, L. J. Hendriks, R. J. Nolte and J. J. Cornelissen, *J. Am. Chem. Soc.*, **131**, 17771 (2009).
42. S. Kang, M. Uchida, A. O'Neil, R. Li, P. E. Prevelige and T. Douglas, *Biomacromolecules*, **11**, 2804 (2010).
43. G. J. Tong, S. C. Hsiao, Z. M. Carrico and M. B. Francis, *J. Am. Chem. Soc.*, **131**, 11174 (2009).
44. C. W. Hung, *RNA packaging and gene delivery using Tobacco mosaic virus pseudo virions*, Ph. D. Thesis, University of Maryland, U.S. (2008).
45. N. Ohtake, K. Niikura, T. Suzuki, K. Nagakawa, S. Mikuni, Y. Matsuo, M. Kinjo, H. Sawa and K. Ijiro, *Chembiochem.*, **11**, 959 (2010).
46. I. J. Minten, V. I. Claessen, K. Blank, A. E. Rowan, R. J. Nolte and J. J. Cornelissen, *Chem. Sci.*, **2**, 358 (2011).
47. J. E. Glasgow, S. L. Capehart, M. B. Francis and D. Tullman-Ercek, *ACS Nano*, **6**, 8658 (2012).
48. B. Jung, A. L. Rao and B. Anvari, *ACS Nano*, **5**, 1243 (2011).
49. R. A. Miller, A. D. Presley and M. B. Francis, *J. Am. Chem. Soc.*, **129**, 3104 (2007).
50. M. Endo, M. Fujitsuka and T. Majima, *Chemistry*, **13**, 8660 (2007).
51. M. T. Klem, M. Young and T. Douglas, *J. Mater. Chem.*, **18**, 3821 (2008).
52. Z. Su and Q. Wang, *Angew. Chem. Int. Ed. Eng.*, **49**, 10048 (2010).
53. Q. Wang, T. Lin, L. Tang, J. E. Johnson and M. G. Finn, *Angew. Chem. Int. Ed.*, **41**, 459 (2002).
54. Q. Wang, T. R. Chan, R. Hilgraf, V. V. Fokin, K. B. Sharpless and M. G. Finn, *J. Am. Chem. Soc.*, **125**, 3192 (2003).
55. N. F. Steinmetz, *Nanomedicine*, **6**, 634 (2010).